مجلة جامعة دمشق للعلوم الهندسية
المجلد 40- العدد 1 (2024) 290-278

Damascus university Journal for engineering sciences
Vol 40 No.1 (2024): 290-278

استخدام الفانتوم الرياضي MIRD5 لحساب الجرعة الممتصة في الأعضاء عند التصوير المحوسب لمنطقتي الدماغ والصدر

عائشه العلي الجوار[1]، د.م. هاني عماشة[2]، أ.د. نقولا أبو عيسى[3]

[1]مهندس – الجامعة السورية الخاصة.

[2]أستاذ مساعد – كلية الهندسة الطبية – جامعة دمشق.

[3]أستاذ – كلية الهندسة الطبية – جامعة دمشق.

الملخص

الهدف: محاكاة الأعضاء وحساب الجرعة الممتصة في كل عضو خلال التصوير المحوسب للدماغ والصدر.

الطرق والمواد: جرى في هذا البحث استخدام النموذج الرياضي MIRD5 للرجل والأنثى البالغة، لحساب توزع الجرعة الإشعاعية الممتصة في الأعضاء الداخلية من الجسم عند التصوير المحوسب لمنطقتي الصدر والدماغ. تم في هذا البحث استخدام النموذج الرياضي MIRD5 إضافة للكود MCNP لمحاكاة أعضاء الجسم ومن ثم حساب مقدار الجرعة الممتصة في كل عضو باستخدام بروتوكولات تصوير الصدر والدماغ، عند قيم الجهد (80 KVp, 100 KVp, 120 KVp).

وجد أنه في حالة التصوير المحوسب للصدر تبلغ الجرعة الإشعاعية قيمة أعظمية في عظام الكتف، والقفص الصدري، والجلد، والذراعين، والصدر، والرئتين. أما في حالة التصوير المحوسب للدماغ، تبلغ الجرعة الإشعاعية قيمة أعظمية في عظام الوجه، والجلد، وعظام الجمجمة، والدماغ، والعمود الفقري، وعظام الكتف.

وتبين أنه مع ازدياد قيمة الجهد تزداد قيمة الجرعة الممتصة، وتكون الجرعة الممتصة لدى الرجل أكبر من مثيلتها لدى المرأة، حيث بلغت قيم هذه الجرع في حالة تصوير الصدر والدماغ على الترتيب القيم التالية:

تاريخ الإيداع: 2022/7/17
تاريخ القبول: 2023/4/25

النموذج	أثناء تصوير الصدر	أثناء تصوير الدماغ
الرجل	$D_{120} = 1.5 \times D_{100}$ $D_{120} = 2 \times D_{80}$	$D_{120} = 1.4 \times D_{100}$ $D_{120} = 2.5 \times D_{80}$
المرأة	$D_{120} = 1.2 \times D_{100}$ $D_{120} = 1.5 \times D_{80}$	$D_{120} = 1.1 \times D_{100}$ $D_{120} = 1.45 \times D_{80}$

المناقشة:

أنَّ اختلاف قيم الجرعة لدى الرجل والمرأة يعود الى اختلاف حجم الأعضاء، حيث تكون بنية الرجل أكبر من بنية المرأة وبالتالي قيم الجرعة لديه أكبر.

نتيجة للتصوير المقطعي المحوسب للدماغ والصدر، من الضروري مراعاة جميع الوسائل اللازمة لخفض جرعة المريض مثل: التدريع بالرصاص للأعضاء السليمة غير الخاضعة للفحص، وضبط الجهد والتيار على قيم منخفضة دون تقليل جودة الصورة.

الكلمات المفتاحية: MCNP، التصوير المقطعي المحوسب CT، فانتوم MIRD، الجرعة الإشعاعية.

Using the MIRD5 Mathematical Phantom to calculate the absorbed dose in organs in case of brain and chest CT scan

Aysha Al-Ali Al-Jewar[1], Dr. Hani Amasha[2], prof. Nikola Abo Issa[3]

[1]Engineer – Syrian Private University − Syria.

[2]Associate professor - Faculty of Biomedical Engineering – Damascus University

[3]professor - Faculty of Technical Engineering - Damascus University .

Received: 17/7/2022
Accepted: 25/4/2023

Abstract

Purpose: Simulate organs and calculate the absorbed dose in each organ for brain and chest CT scans.

Method and Materials: In this research; the mathematical phantom MIRD5 for adult men and women was used to calculate the absorbed dose in organs, in the case of brain and chest CT scans. Where; the mathematical phantom MIRD5 and MCNP code were used to simulate organs and calculate the absorbed dose in each organ for brain and chest CT scans, in Voltage (80 KVp, 100 KVp, 120 KVp).

Results:

For chest scan, the maximum absorbed dose was in scapulae, rib cage, skin, arm bones, breasts, and lungs. For brain scan, the maximum absorbed dose was in the facial skeleton, skin, cranium, Brain, Spine, and scapulae.

With the increase in the value of Voltage, the value of the absorbed dose increases, and the absorbed dose in men is greater than the dose in women.

- For the man's phantom during chest imaging, we find:

$$D_{120} = 1.5 \times D_{100} \quad , \quad D_{120} = 2 \times D_{80}$$

- For the woman's phantom during chest imaging, we find:

$$D_{120} = 1.2 \times D_{100} \quad , \quad D_{120} = 1.5 \times D_{80}$$

- For the man's phantom during brain imaging, we find:

$$D_{120} = 1.4 \times D_{100} \quad , \quad D_{120} = 2.5 \times D_{80}$$

- For the woman's phantom during brain imaging, we find:

$$D_{120} = 1.1 \times D_{100} \quad , \quad D_{120} = 1.45 \times D_{80}$$

Conclusion: The difference in the dose values for men and women is due to the difference in the size of the organs, where the structure of the man is larger than the structure of the woman and therefore the values of the dose for the man are larger.

As a result, for CT chest scan and brain scan, it is necessary to consider all means necessary to reduce the patient's dose such as: lead shielding of healthy organs not subject to scan, and setting voltage and current to low values without reducing image quality.

Key Words: MCNP, CT scan, MIRD phantom, Radiation Dose

First: Introduction

Despite the many parameters used to estimate radiation exposure from CT imaging devices, such as the volumetric dose index, and the dose-length DLP product that describes the radiation output of the imaging device, they are not able to characterize the dose received by each patient [1].

The radiation dose of X-rays resulting from CT scanners has become an important topic as a result of the large numbers of examinations carried out using these devices around the world [2]. According to ref.[2] ,the number of annual CT examinations in the United States rose from 2.8 million examinations in 1981 to 20 million examinations annually in 1995 to and then to 62 million examinations in 2007, and in Germany between 1996 and 2012, the annual effective dose resulting from Computerized imaging examinations doubled, and the number of examinations in Italy increased between 2004 and 2014 by 39% per 1000 population [2]. Table (1) shows a comparison between the effective dose obtained from CT scans with each of the numbers of images of conventional chest imaging and the number of years of exposure to natural background rays, which produces the same effective dose obtained from CT scans [12].

Table (1) Comparison between the effective dose resulting from CT scan with each of the numbers of images of conventional chest imaging and the number of years of exposure to natural background rays, which produces the same effective dose resulting from CT.

number of years of exposure to natural background rays	numbers of images of conventional chest imaging	Effective Dose	Imaging protocol
CT scan of the head	2.3	115	1 Year
CT scan of the chest	8	400	3.6 Years
CT scan of the abdomen and pelvis	10	500	4.5 Years

Until now, several computer applications have been presented for calculating the dose of organs in computerized imaging, and each of them differs from the other according to the phantom used, the algorithms adopted in the calculation, the approved reference device...etc. Among these applications:

CT-Expo was designed by German researchers using Excel. This application uses a family of mathematical phantoms (Adam, Eva, Child, Baby) which are built utilizing mathematical equations that describe the surface of each member of the body. Imaging (axial-helical) [2]

Application (NCICTX) relative to the National Cancer Institute CT used elemental volumetric phantoms based on reading and segmentation of medical images CT. The application contains a wide range of families of phantoms of different sizes [2].

In (2020), Markus et al., calculated the absorbed and effective dose for different organs of the human body using phantoms for adult women and adult men based on Monte Carlo simulation methods [1].

Table (2) The absorbed and effective dose for different organs in ref. [1].

Organs	Equivalent organ dose [mGy]	W_T	Effective organ dose (female) [mSv]	Effective organ dose (male) [mSv]	C_{ORGAN} (female)	C_{ORGAN} (male)
Red bone marrow	12.3 (±2.3)	0.12	1.49 (±0.24)	1.47 (±0.28)	0.125	0.126
Colon	11.2 (±2.8)	0.12	1.28 (±0.08)	1.36 (±0.38)	0.108	0.116
Lung	13.4 (±1.9)	0.12	1.48 (±0.15)	1.64 (±0.38)	0.125	0.14
Stomach	12.2 (±1.5)	0.12	1.39 (±0.06)	1.48 (±0.23)	0.117	0.127
Breast	10.9 (±0.8)	0.12	1.30 (±0.09)		0.11	
Gonads	14.6 (±4.1)	0.08	0.74 (±0.07)	1.29 (±0.26)	0.063	0.111
Bladder	11.7 (±2.0)	0.04	0.40 (±0.05)	0.49 (±0.06)	0.034	0.042
Liver	12.0 (±1.2)	0.04	0.46 (±0.04)	0.49 (±0.08)	0.039	0.042
Esophagus	11.1 (±1.4)	0.04	0.42 (±0.05)	0.45 (±0.01)	0.035	0.039
Thyroid gland	21.2 (±3.2)	0.04	0.90 (±0.04)	0.83 (±0.05)	0.076	0.071
Skin	11.0 (±2.1)	0.01	0.09 (±0.00)	0.11 (±0.03)	0.08	0.01
Bone surface	26.6 (±4.7)	0.01	0.24 (±0.01)	0.27 (±0.03)	0.02	0.023
Salivary glands	14.3 (±2.8)	0.01	0.12 (±0.01)	0.15 (±0.03)	0.01	0.013
Brain	12.7 (±3.3)	0.01	0.10 (±0.00)	0.14 (±0.03)	0.08	0.012

And in (2017), Abu shaded et al., studied the absorption dose distribution resulting from chest imaging at different X-ray tube voltages using the mathematical phantom [13].

Table (3) Absorbed dose in parts of the heart muscle, chest, stomach wall, thyroid gland, kidneys and lungs for voltage values (120, 100, 80) kVp.

Organ	Absorbed Dose [m Gy]		
	80 KVp	100 KVp	120 KVp
Heart	9.11	21.86	36.99
Breast	2.03	3.90	6.22
Stomach wall	0.30	0.67	1.16
Thyroid	0.78	1.66	2.79
Kidney	0.10	0.28	0.52
Liver	0.45	1.02	1.75
Right Lung	1.58	3.29	5.45
Left Lung	1.60	3.16	5.28

Second: Radiation Dose in Computed Tomography:

[2.1] Radioactive dose absorbed in tissues:

The spectrum of X-rays used in radiological diagnosis under 150 kV has a peak that turns into secondary electrons when it passes through the tissue. It has a range of less than 0.28 mm in soft tissues, 0.16 mm in

cortical bone, 1.1 mm in lung tissue, 0.26 mm in the skin [3]. Since the probability of producing Bremsstrahlung braking rays is very low, it is assumed that the energy of the secondary electrons produced is completely absorbed in the interaction

regions [3], which is known as the kerma approximation principle.

[2.2] Effective dose and weighting factors

The biological effects of radiation on tissues are not only related to the dose provided to the tissue or organ but also depend on the biological sensitivity of the tissue or organ exposed to radiation X-ray body.

The effective dose is estimated in one Sievert (Sv) or its parts, and it is calculated in two ways [4]:

The first method depends on calculating the absorbed dose in the different organs of the body or the equivalent of these organs within a hermaphroditic mathematical phantom, either practically or using Monte Carlo methods:

$$\text{Effective dose} = \sum \text{Dose}_{\text{tissue}} \times \text{Weighting factor}_{\text{tissue}} \dots\dots (1)$$

Weighted tissue parameters are given according to the publications of the International Committee on Radiological Protection ICRP 26 [1977], ICRP 60 [1991], and ICRP 103 [2007] as shown in Figure (2):

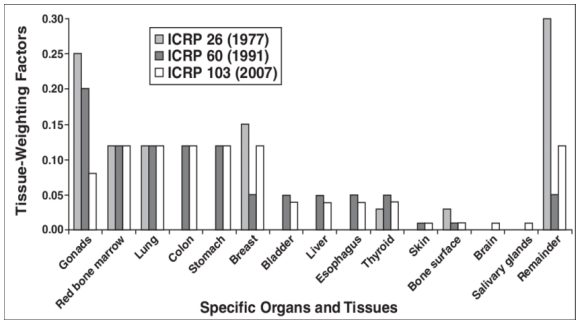

Figure (2) Weighted tissue parameters for different organs and tissues according to the reports of the International Committee on Radiological Protection 26 [1977], 60 [1991], 103 [2007]

Or the effective dose is estimated based on knowledge of both the dose product-length DLP and tabulated conversion factors according to the relationship:

$$\text{Effective dose} = \text{DLP} \times \text{k coefficients} \dots (2)$$

The values of the k-factor are estimated through several CT scans and depending on the reference patient, and it varies with age, weight, and gender. Table (4) shows the values of the k parameter according to the age and the area under examination [12]:

Table (4) Effective dose factor values for adults and children (according to the British study 2003)

The imaged area of the body	Effective dose factor values [$mSv \cdot (mGy \cdot cm)^{-1}$]				
	Less than 1 year	1 year	5 years	10 years	adults
head	0.011	0.0067	0.0040	0.0032	0.0021
chest	0.039	0.026	0.018	0.013	0.014
Belly	0.049	0.030	0.020	0.015	0.014
pelvis	0.049	0.030	0.020	0.015	0.015

Third: The materials used in the study:

[3.1] Code MCNP The Monte Carlo N-Particle

This code was developed in Los Alamos laboratories in the United States of America, starting in the 1940s, as it is characterized by the possibility of modeling complex three-dimensional structures, and it also uses continuous energy atomic and nuclear cross-sectional interaction libraries. It depends on random methods based on probability and deals with the fate of a large number of particles separately, as it calculates the median paths for each particle from the sample and then gives the final result for one particle with an arithmetic error.

Therefore, the greater the number of studied particles, the lower the value of the error, [5]. This code was written in the FORTRAN language and runs on an MS-DOS system. It needs an input file that is written manually and linked with the boot file of the code mcnpx.exe via the Windows system command prompt cmd.exe to perform the necessary calculations. The latest version of the MCNPX-2.3.0 code include a library of cross section of all charged and uncharged particles (protons, alpha particles, electrons, neutrons, etc.) in addition to gamma rays.

[3.2] Computational phantom

The mathematical phantom was used to simulate the interaction of different ionizing rays with the organs of the human body using Monte Carlo methods [6]. This phantom includes accurate anatomical information of the human body and is similar in composition to the density and chemical composition of important organs in the human body.

The first model of this type of phantoms was created in the sixties of the last century, where was relied in his design on simple geometric shapes

such as cylinders, ellipses, and conical shapes, which were used to form phantoms for adults and others for children. In the 1970s, the first structurally differentiated model, was designed which was used to measure internal doses in nuclear medicine (Medical Internal Radiation Dose (MIRD)), using the anatomical information of the reference man recommended by the International Commission on Radiological Protection (ICRP).Where the body and members were simulated using simple geometric shapes such as planes, segments, and cylinders described according to mathematical equations that determine the shape of each member [7]. Three main regions can be distinguished in terms of density in this phantom: skeletal, soft tissue, and lung. Table (5) gives the chemical composition and density of each tissue for all types of phantoms (except for the newborn child) [8].

Table (5) The composition of the different tissues involved in the composition of the phantoms, except for the newborn child [8]

Element	Percent by weight		
	Soft tissue	Skeleton	Lung
H	10.454	7.337	10.134
C	22.663	25.475	10.238
N	2.490	3.057	2.866
O	63.525	47.893	75.752
F	0	0.025	0
Na	0.112	0.326	0.184
Mg	0.013	0.112	0.007
Si	0.030	0.002	0.006
P	0.134	5.095	0.080
S	0.204	0.173	0.225
Cl	0.133	0.143	0.266
K	0.208	0.153	0.194
Ca	0.024	10.190	0.009
Fe	0.005	0.008	0.037
Zn	0.003	0.005	0.001
Rb	0.001	0.002	0.001
Sr	0	0.003	0
Zr	0.001	0	0
Pb	0	0.001	0
Density	1.04 g/cm^3	1.4 g/cm^3	0.296 g/cm^3

The phantom is drawn on the z-axis upward so that the coordinate principle is located exactly in the middle of the base of the trunk and the x-axis passes through the left part of the phantom. The members and the distances between the different members are represented in geometric shapes through mathematical equations, where the dimensions are entered in centimeters and with an accuracy of 1/100, two numbers after the decimal point.

We will represents some examples of how we can create some organs using the MCNP code:

Trunk area

The torso in this phantom (excluding the breasts) is represented by a stereotype of a cylinder with an ellipse (ellipse) given by the two equations:

$$\left(\frac{x}{A_T}\right)^2 + \left(\frac{y}{B_T}\right)^2 \le 1 \;;\quad 0 \le z \le C_T \ldots (3)$$

The values of the constants in the eq. 3 in addition to the volume and mass of the area are given in Table (6):

Table (6) the values of the constants, the size, and mass of the trunk according to age

Phantom	Length (cm)			Volume (cm^3)	Mass (g)
	A_T	B_T	C_T		
Newborn	6.35	4.90	21.60	2,110	2,100
Age 1	8.80	6.50	30.70	5,520	5,530
Age 5	11.45	7.50	40.80	11,000	11,000
Age 10	13.90	8.40	50.80	18,600	18,700
15-AF	17.25	9.80	63.10	33,500	34,500
Adult male	20.00	10.00	70.00	44,000	44,800

Head area

The head area with the neck is expressed by several cylindrical and segmental solids and is represented using the following equations:

$$x^2 + y^2 \le R_H^2 \;;\; C_T \le z \le C_T + C_{HO} \ldots . (4)$$

$$\left(\frac{x}{A_H}\right)^2 + \left(\frac{y}{B_H}\right)^2 \le 1 \;;\quad C_T + C_{HO} \le z \le C_T + C_{HO} + C_{HI} \ldots (5)$$

Table (7) values of the constants, head size, and mass by age

Phantom	Length (cm)						Volume (cm^3)	Mass (g)
	R_H	A_H	B_H	C_{HO}	C_{H1}	C_{H2}		
Newborn	2.8	4.52	5.78	1.56	7.01	3.99	965	1,020
Age 1	3.6	6.13	7.84	2.30	9.50	5.41	2,410	2,580
Age 5	3.8	7.13	9.05	3.30	10.70	6.31	3,670	4,000
Age 10	4.4	7.43	9.40	4.70	11.68	6.59	4,300	4,710
15-AF	5.2	7.77	9.76	7.70	12.35	6.92	4,900	5,410
Adult male	5.4	8.00	10.00	8.40	13.05	7.15	5,430	6,040

Fourth: Research Methodology:

1. Description the mathematical equations that describe the different members,
2. Depending on the mathematical equations of human organs, the MIRD5 phantom using MCNP code was created.
3. The composition of the different tissues of the phantom was selected according to table 5.
4. The X-ray source was modeling using the SDEF card available in MCNP code as cylindrical surface with a height equivalent to the thickness of the slice.
5. Source surface distance SSD was adapted equal to 60 cm.

6. To calculate the average energy deposited within a specific cell (specific organ) in unit of (MeV/g), the F6 card was used, this card gives the energy deposited in the unit of mass, which is given by the relationship:

$$DE\left(\frac{MeV}{g}\right) = W \times T_l \times \sigma_T(E) \times H(E) \times \frac{\rho_a}{m} \ldots\ldots (6)$$

where: W is the source weight, T_l is the particle track length (cm),

$\sigma_T(E)$: the total microscopic cross-section in barns,

H(E): heating number in MeV/collision,

ρ_a: the atomic density of the cell substance (atoms/barns.cm), m: the mass of the cell (g).

And from it the value of the absorbed dose in each cell, estimated in one (Gy = J/kg) is calculated by the relationship:

$$D\left(\frac{Gy}{\text{source particle}}\right) = DE\left(\frac{MeV}{g}\right) \times 1.6 \times 10^{-13}\left(\frac{J}{MeV}\right) \times 10^{3}\left(\frac{g}{kg}\right) \ldots (7)$$

Since in the MCNP code, the dose was for a single particle, the normalization factor is used, which represents the total number of photons emitted per unit current-time (Photon/mAs) at a given voltage of the X-ray tube

Table (8) The normalization factor values used in some reference studies

Normalization Factor (particle/mAs)			KVp
Ref.[9]	**Ref.[10]**	**Ref.[13] Slice Thickness=10 mm**	
4.18×10^{13}	2.53×10^{11}	3.66×10^{11}	**80**
5.83×10^{13}	3.96×10^{11}	4.50×10^{11}	**100**
7.65×10^{13}	4.12×10^{11}	5.37×10^{11}	**120**
9.50×10^{13}	-	6.48×10^{11}	**140**

Fifth: Results and Discussion:

The MCNP code provides the ability to visualize the distribution of the studied particles within the different cells according to the source description. Therefore, this feature was used to display the distribution of X-ray photons during imaging across the cells of the studied model, Figure (3).

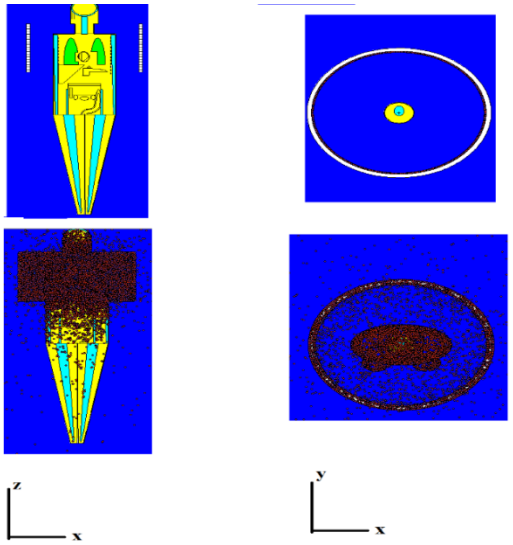

Figure (3) The distribution of X-ray photons within the phantom of an adult woman when computerized to the chest area, where the length of the scan area L=37 cm (34 cm to 71 cm) and the voltage is 80 kVp

[5.1] Radiation dose in organs

The imaging process of the chest and head regions were simulated according to the following imaging protocols [11]:

Table (9) Imaging protocols adopted when examining the chest and head.

ROUTINE AXIAL BRAIN	ROUTIN E CHEST	SCAN NAME
Axial	Helical	Scan Type
120kv / 480 mA / .5 sec	120kv / smart mA (120-450) / 0.5 sec	KV/mA/ Rotation time (sec)
	1.375:1 , 27.50mm	Pitch / Speed (mm/rotation)
Skull base- Skull vertex DFOV=25 cm decrease appropriately	1cm superior to lung apices through adrenal glands DFOV=38 cm	Scan Start / End Locations

In the simulation, we adopted the values of the regularization coefficients presented in Table (6), that is, the doses were calculated for each 1 mAs. Figure (4), Figure (5), and Figure (6) show the value of the absorbed radiation dose in organs estimated in one [Gy/1 mAs] when CT scan of the chest area using the adult woman and adult man model, while Figure (7), Figure (8), and Figure (9) show the value of the absorbed radiation dose in Organs are estimated in one [Gy/1 mAs] when CT

scan of the head region using the adult woman and adult man model.

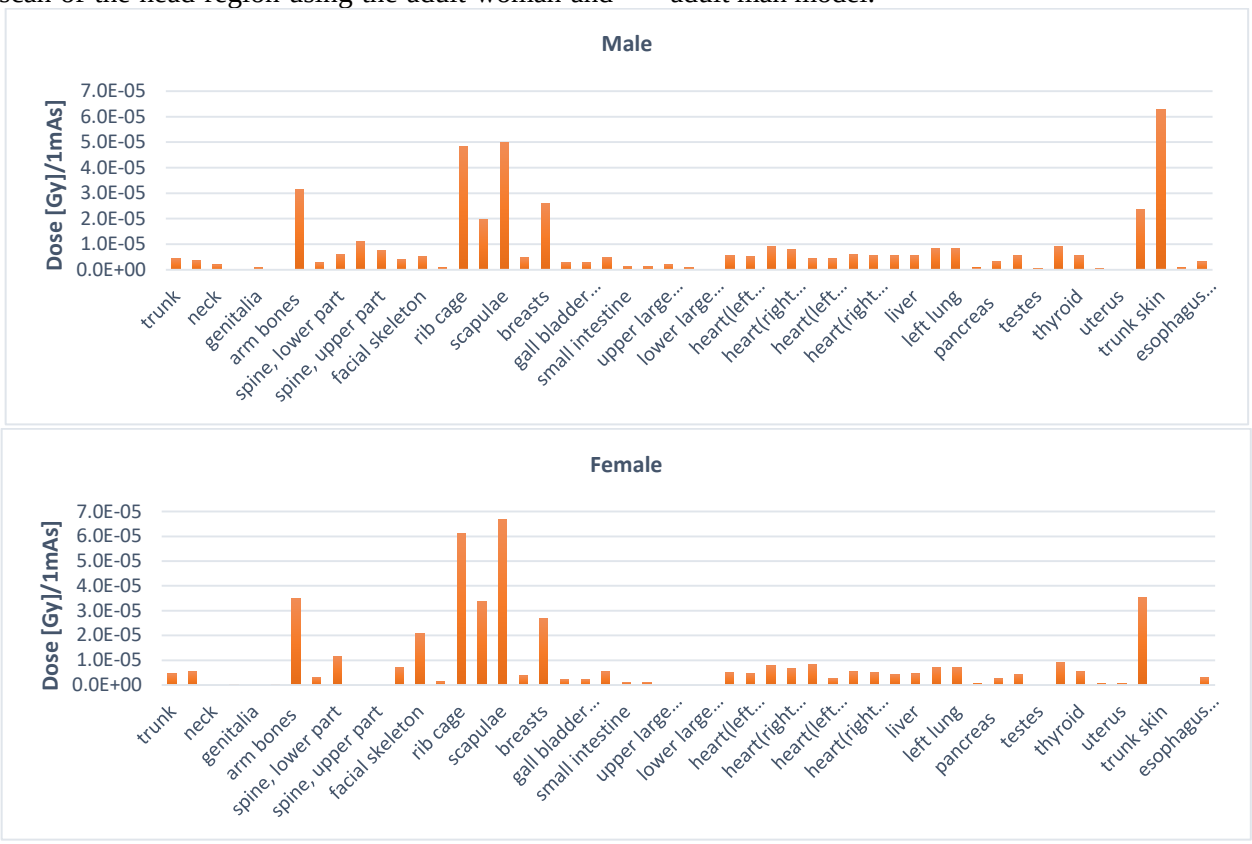

Figure (4) Radiation dose absorbed into organs when computerized imaging of the chest area (80 KVp)

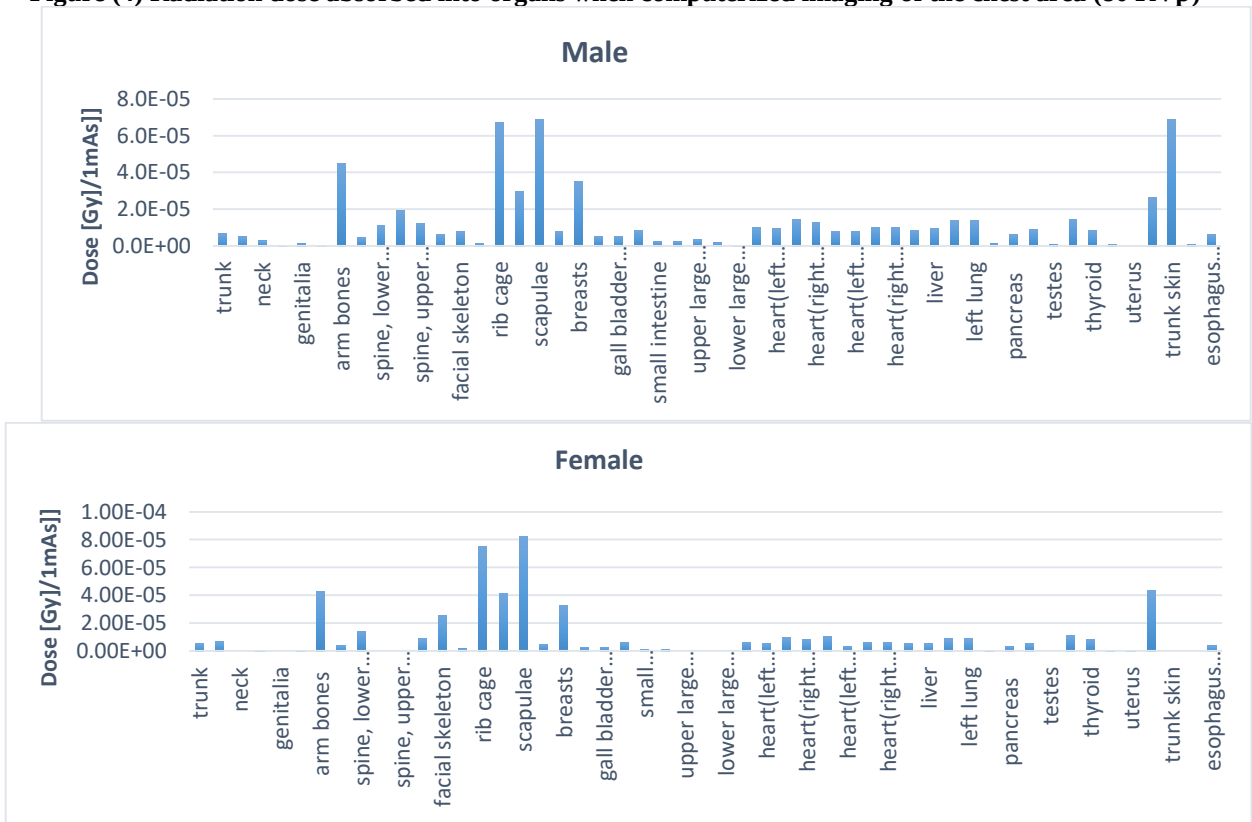

Figure (5) Radiation dose absorbed into organs when computerized imaging of the chest area (100 KVp)

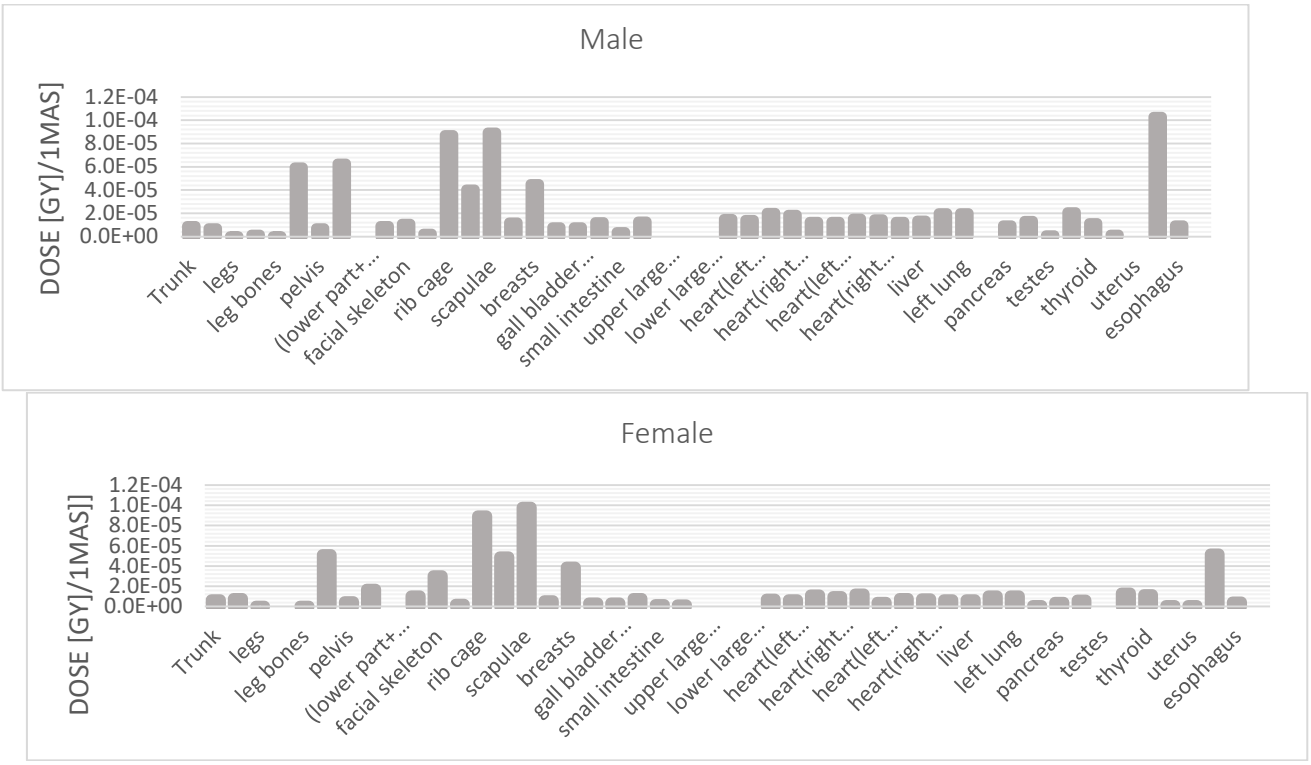

Figure (6) Radiation dose absorbed into organs when computerized imaging of the chest area (120 KVp)

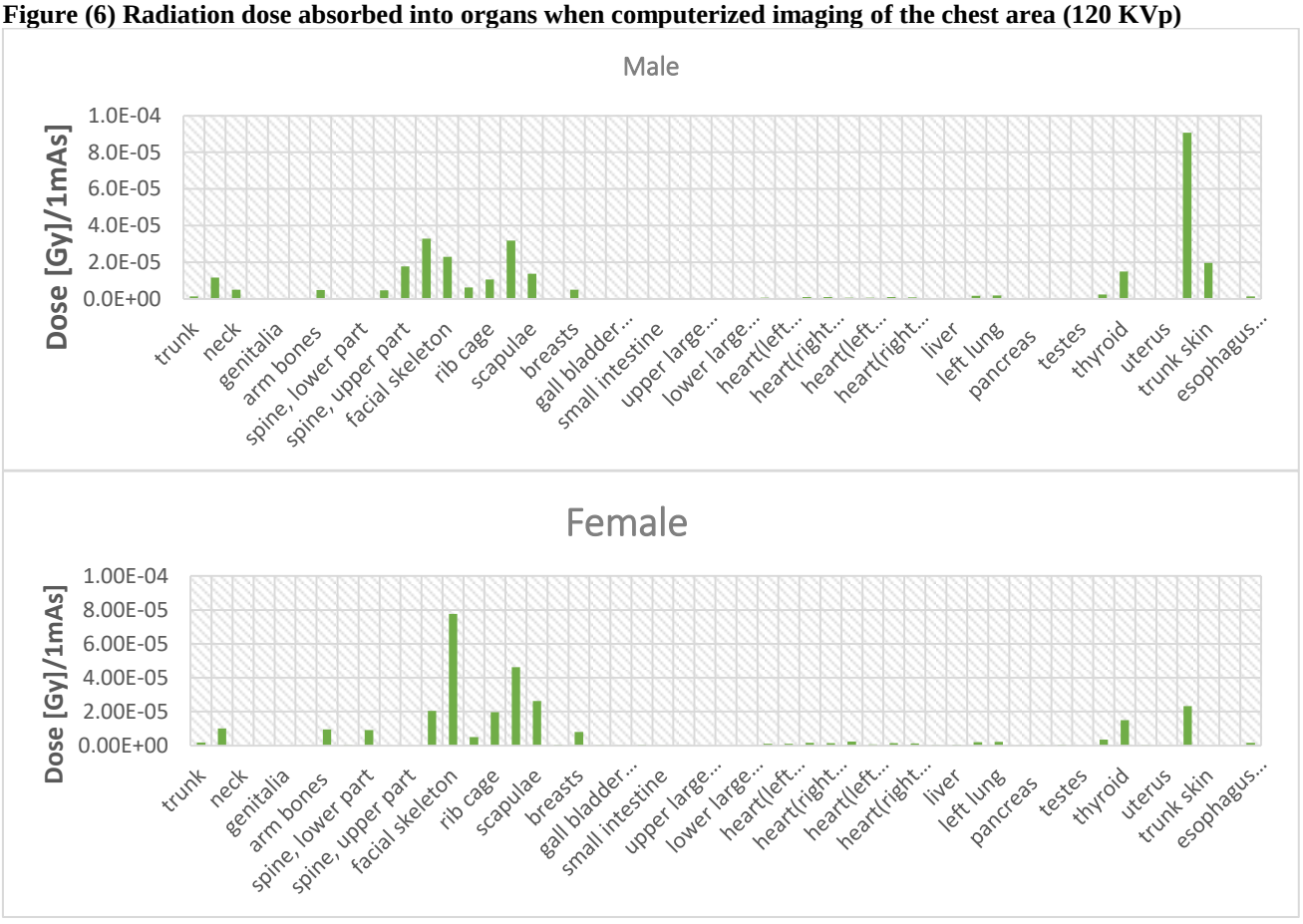

Figure (7) The absorbed radiation dose in the organs when computerized imaging of the brain (80 KVp)

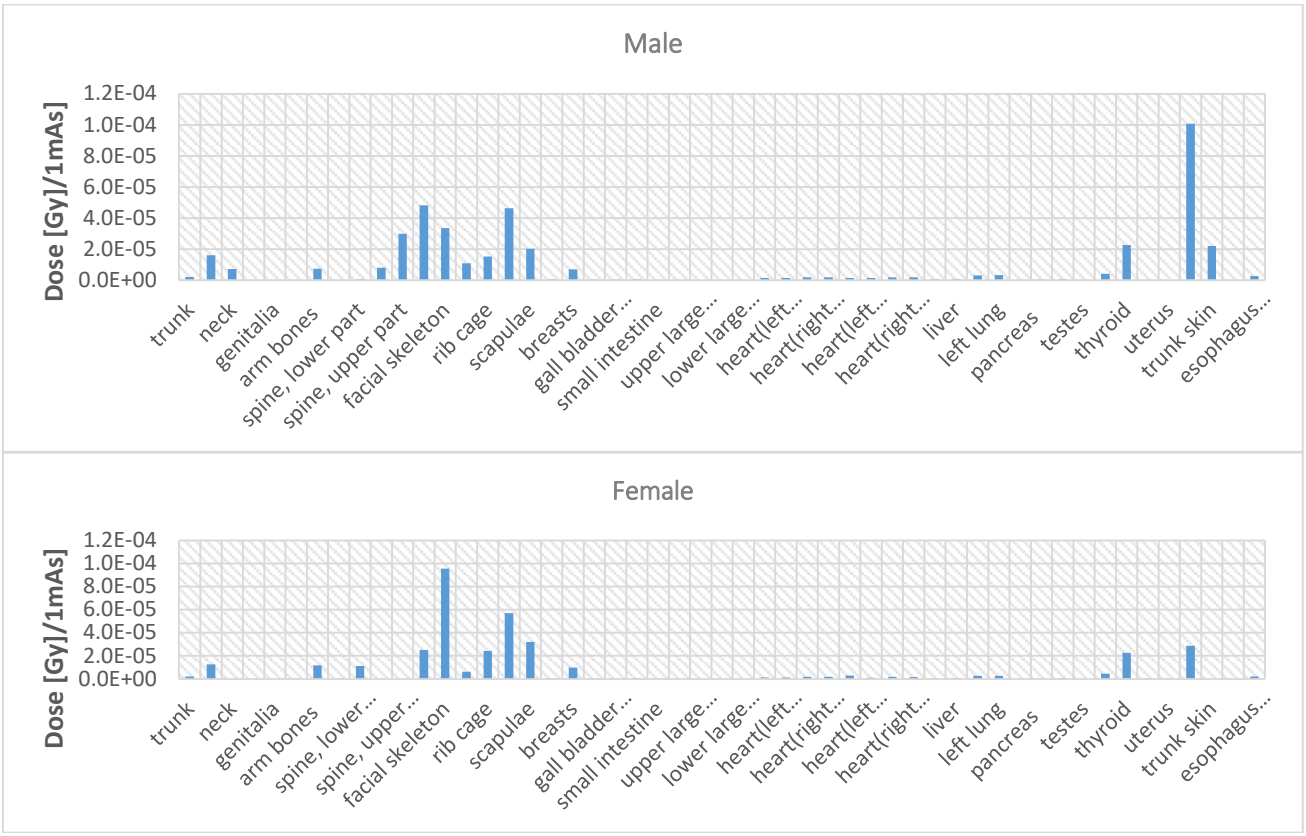

Figure (8) The absorbed radiation dose in the organs when computerized imaging of the brain (100 KVp)

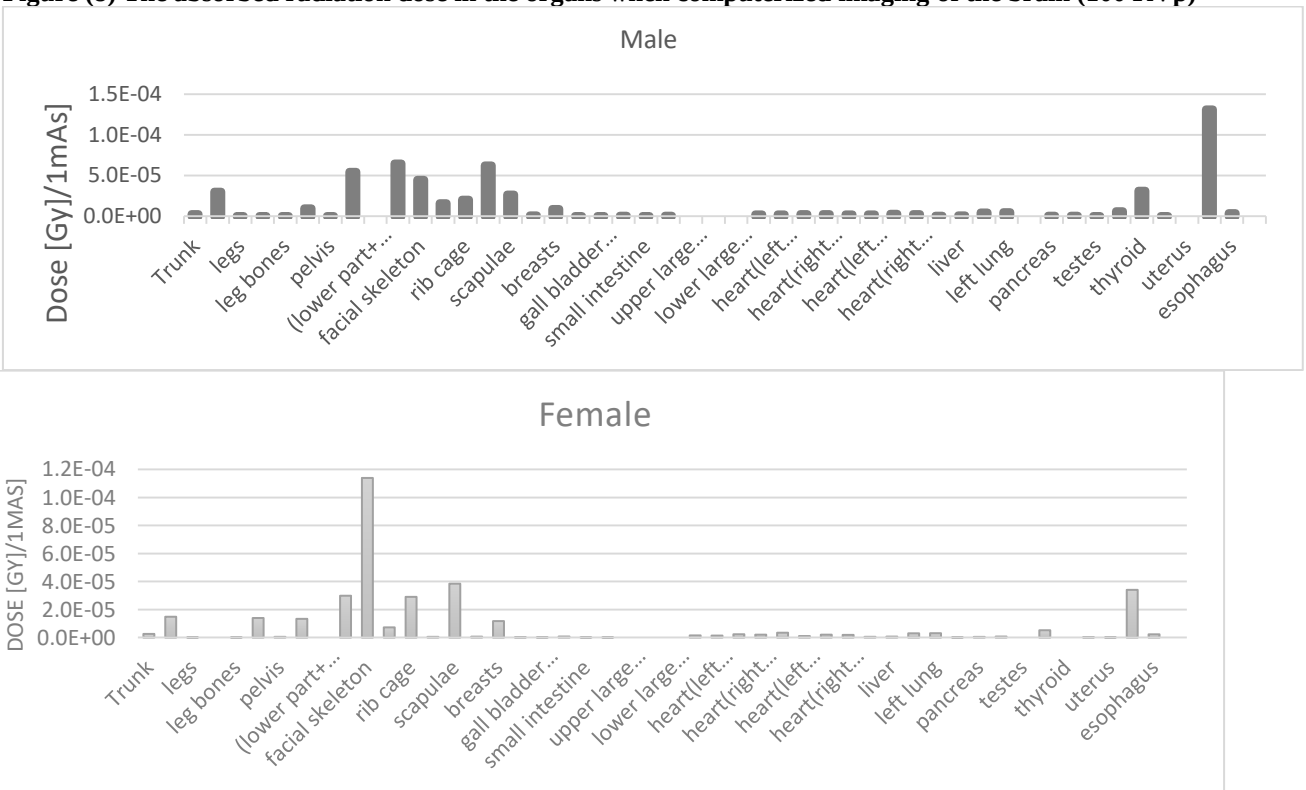

Figure (9) The absorbed radiation dose in the organs when computerized imaging of the brain (120 KVp)

[5.2] Discussion of Results:

From Figures (4,5,6), we found that the absorbed dose in the case of chest scan for adult woman reaches maximum values in the shoulder bones, followed by the bones of the chest cage, collarbone, skin, arms, breasts, where the dose in these parts exceeds the value $4 \times 10^{-5} \frac{\text{Gy}}{\text{1mAs}}$

For internal organs, the dose absorbed in the heart is $6.68 \times 10^{-5} \frac{\text{Gy}}{\text{1mAs}}$, In the liver $6.50 \times$

$10^{-6}\frac{\text{Gy}}{1\text{mAs}}$, the lungs $2.09\times10^{-5}\frac{\text{Gy}}{1\text{mAs}}$, in the womb $9.01\times10^{-7}\frac{\text{Gy}}{1\text{mAs}}$, the brain $2.01\times10^{-6}\frac{\text{Gy}}{1\text{mAs}}$.

While the absorbed radiation dose in the case of chest scan in the case of an adult man reaches maximum values in the skin, shoulder bones, chest bones, spine, collarbone, and arms, where the absorbed radiation dose in the skin exceeds the value $1\times10^{-4}\frac{\text{Gy}}{1\text{mAs}}$.

For sensitive internal organs, the dose absorbed in the heart is $1.24\times10^{-4}\frac{\text{Gy}}{1\text{mAs}}$, In the liver $1.39\times10^{-5}\frac{Gy}{1mAs}$, the lungs $4.03\times10^{-5}\frac{\text{Gy}}{1\text{mAs}}$, in the testes $1.17\times10^{-6}\frac{\text{Gy}}{1\text{mAs}}$, the brain $2.50\times10^{-6}\frac{\text{Gy}}{1\text{mAs}}$.

While in the case of brain scan, Figures (7,8,9), we found that the value of the absorbed radiation dose when imaging the brain in the case of an adult woman reaches maximum values in the bones of the face, shoulder bones, skin, brain, and skull bones.

The sensitive dose is $7.31\times10^{-6}\frac{Gy}{1mAs}$ in the brain, $1.62\times10^{-5}\frac{Gy}{1mAs}$ in the heart, in the lungs $6.74\times10^{-6}\frac{Gy}{1mAs}$, and in the womb $9.28\times10^{-8}\frac{Gy}{1mAs}$. For sensitive internal organs in men, the dose absorbed in the brain is $1.62\times10^{-5}\frac{Gy}{1mAs}$, the heart is $2.07\times10^{-5}\frac{Gy}{1mAs}$, the lungs are $9.53\times10^{-6}\frac{\text{Gy}}{1\text{mAs}}$, and in the testes $1.35\times10^{-7}\frac{\text{Gy}}{1\text{mAs}}$.

With the increase in the value of Voltage, the value of the absorbed dose increases, and the absorbed dose in men is greater than the dose in women.

- For the man's phantom during chest imaging, we find:

$$D_{120}=1.5\times D_{100}$$

$$D_{120}=2\times D_{80}$$

- For the woman's phantom during chest imaging, we find:

$$D_{120}=1.2\times D_{100}$$

$$D_{120}=1.5\times D_{80}$$

- For the man's phantom during brain imaging, we find:

$$D_{120}=1.4\times D_{100}$$

$$D_{120}=2.5\times D_{80}$$

- For the woman's phantom during brain imaging, we find:

$$D_{120}=1.1\times D_{100}$$

$$D_{120}=1.45\times D_{80}$$

When comparing the dose value between men and women in chest imaging:

$$D_{120M}=0.7\times D_{120F}$$

$$D_{100M}=0.8\times D_{100F}$$

$$D_{80M}=1.1\times D_{80F}$$

When comparing the dose value between men and women in Brain imaging:

$$D_{120M}\approx D_{120F}$$

$$D_{100M}=1.1\times D_{100F}$$

$$D_{80M}=1.3\times D_{80F}$$

$D_{(number)M}$: D is Absorbed Dose, (number) is the Voltage Value, M for Male.

$D_{(number)F}$: D is Absorbed Dose, (number) is the Voltage Value, F for Female.

By comparing our results from the chest rendering with the corresponding results from the reference study [13], we find the deviation values from the reference level as shown in Table (10), and the reason for the deviation in the values is explained by using a different phantom than the phantom used in our MIRD 5 study.

Table (10), Deviation ratio with ref. [13].

Organ	Deviation ratio with ref [13].		
Heart	**80 KVp**	**100 KVp**	**120 KVp**
Breast	-12%	-60%	-65%
Stomach wall	19%	1%	-25%
Thyroid	-5%	-40%	-51%

Kidney	19%	43%	31%
Liver	12%	9%	-5%
Right Lung	-10%	-49%	-56%
Left Lung	-11%	-48%	-54%

That is, the dose values for men are greater than for women (due to the difference in the size of the organs exposed to radiation). The choice of the scanner voltage (and thus the energy of the photons) is one of the important factors in the dose received by the patient as a result of the interaction of the photons with the tissue. 0.5×0.34=0.17 or 17% of the photons will be displaced from the beam as a result of the interaction, and at photons energy of 100 keV, where the attenuation coefficient is 0.161 cm-1, only about 8% of the photons will be attenuated when they pass through this layer of tissue, Therefore, low-energy X-rays will be better at producing an image with a clear contrast in this layer of tissue. These results are also valid for tissues with high atomic numbers (such as bones).

On the other hand, using a high voltage (high photon energy) will result in a lower entry dose (skin dose) compared to the internal organs dose for a specific protocol.

Therefore, it is always necessary to reconcile in obtaining medical images that are acceptable in terms of diagnosis, with the need to reduce the dose received by the patient to the lowest possible from the point of view of radiation protection.

Funding information: this research is funded by Damascus university – funder No. (501100020595).

References المراجع

1. Kopp, M., Loewe, T., Wuest, W., Brand, M., Wetzl, M., Nitsch, W., . . . May, M. (2020). Individual calculation of effective dose and risk of malignancy based on Monte Carlo simulations after whole body computed tomography. *Scientific Reports, 10*(1). doi:10.1038/s41598-020-66366-2
2. De Mattia, C., Campanaro, F., Rottoli, F., Colombo, P. E., Pola, A., Vanzulli, A., & Torresin, A. (2020). Patient organ and effective dose estimation in CT: Comparison of four software applications. *European Radiology Experimental, 4*(1). doi:10.1186/s41747-019-0130-5
3. R Kramer, H J Khoury and J W Vieira. CALDose_X – a software tool for the assessment of organ and tissue absorbed doses, effective dose and cancer risks in diagnostic radiology.Physics in Medicine and Biology, doi:10.1088/0031-9155/53/22/011.
4. Liang, Q. (2013). *A dissertation submitted in partial fulfillment of the requirements for the degree of Doctor of Philosophy: Patient-specific CT dose determination from CT images using Monte Carlo simulations* (Master's thesis, University of Wisconsin-Madison). University of Wisconsin-Madison.
5. X-5 Monte Carlo Team. April 24, 2003. MCNP — A General Monte Carlo N- Particle Transport Code, Version 5. Volume I: Overview and Theory. Los Alamos National Laboratory، LA-UR-03-1987 (April 24, 2003).
6. X-5 Monte Carlo Team. April 24, 2003. MCNP — A General Monte Carlo N- Particle Transport Code, Version 5. Volume II: User's Guide. Los Alamos National Laboratory، LA-CP-03- 0245 (April 24, 2003).
7. Lee, D. (2012). *Simulation and analysis of human phantoms exposed to heavy charged particle irradiations using the particle and heavy ion transport system (PHITS)* (Master's thesis, 2012). College Station, TX: Texas A & M University.

8. Center for Radiation Protection Knowledge. **Description of the mathematical phantoms**. [Internet]. Available from: http://crpk.ornl.gov/resources/Mird.pdf. [accessed 22.05.01]..
9. Velayudham Ramasubramanian Poonam Yadav .Validation of Radiation Dose from a four slice CT scanner using Monte Carlo .USA : Scholars Research Library: (http://scholarsresearchlibrary.com/archive.html) .ISSN 0975-508X .(2011)
10. C. H. Cagnon, D. D. Cody, D. M. Stevens, C. H. McCollough J. J. DeMarco. A Monte Carlo based method to estimate radiation dose from multidetector CT (MDCT): cylindrical and anthropomorphic phantoms .IOPscience (http://iopscience.iop.org/0031-9155/50/17/005 .(Phys. Med. Biol. 50 3989 ،(2005)،
11. CT Scan (Computed Tomography/CAT Scan), website available on: www.lifespan.org/centers-services/ct-scan-computed-tomographycat-scan/ct-protocols. Accessed at [14/4/20] 1:30 AM.

12. د .م ح خريطة، خ م والي .2010 .إجراء مسح تطبيقي لقياس جرعة المريض في جهاز التصوير الطبقي المحوسب مع التركيز بشكل خاص على جرعة الأطفال .دمشق : هيئة الطاقة الذرية السورية، قسم الوقاية والأمان2010.
13. أبو شديد، توفيق.، نحيلي، ماجدة.، أبو عيسى، نقولا.، (2017). تعيين نسبة الكالسيوم باستعمال الكودات الحاسوبية في أجهزة التصوير الطبقي المحوري المحوسب (رسالة دكتوراه، 2017) جامعة دمشق.